

## THE ABUNDANCE OF STAR-FORMING GALAXIES IN THE REDSHIFT RANGE 8.5 TO 12: NEW RESULTS FROM THE 2012 HUBBLE ULTRA DEEP FIELD CAMPAIGN

RICHARD S ELLIS<sup>1</sup>, ROSS J MCLURE<sup>2</sup>, JAMES S DUNLOP<sup>2</sup>, BRANT E ROBERTSON<sup>3</sup>, YOSHIKI ONO<sup>4</sup>, MATT SCHENKER<sup>1</sup>, ANTON KOEKEMOER<sup>5</sup>, REBECCA A A BOWLER<sup>2</sup>, MASAMI OUCHI<sup>4</sup>, ALEXANDER B ROGERS<sup>2</sup>, EMMA CURTIS-LAKE<sup>2</sup>, EVAN SCHNEIDER<sup>3</sup>, STEPHANE CHARLOT<sup>7</sup>, DANIEL P STARK<sup>3</sup>, STEVEN R FURLANETTO<sup>6</sup>, MICHELE CIRASUOLO<sup>2,8</sup>

*Draft version November 6, 2012*

### ABSTRACT

We present the results of the deepest search to date for star-forming galaxies beyond a redshift  $z \simeq 8.5$  utilizing a new sequence of near-infrared Wide Field Camera 3 images of the Hubble Ultra Deep Field. This ‘UDF12’ campaign completed in September 2012 doubles the earlier exposures with WFC3/IR in this field and quadruples the exposure in the key F105W filter used to locate such distant galaxies. Combined with additional imaging in the F140W filter, the fidelity of all high redshift candidates is greatly improved. Using spectral energy distribution fitting techniques on objects selected from a deep multi-band near-infrared stack we find 7 promising  $z > 8.5$  candidates. As none of the previously claimed UDF candidates with  $8.5 < z < 10$  is confirmed by our deeper multi-band imaging, our campaign has transformed the measured abundance of galaxies in this redshift range. We do, however, recover the candidate UDFj-39546284 (previously proposed at  $z=10.3$ ) but find it undetected in the newly added F140W image, implying either it lies at  $z=11.9$  or is an intense line emitting galaxy at  $z \simeq 2.4$ . Although we cannot formally exclude the latter hypothesis without a spectrum, we argue that such an explanation is unlikely. Despite the uncertain nature of this source, our new, robust  $z \simeq 8.5 - 10$  galaxy sample indicates that the luminosity density broadly continues the smooth decline observed over  $6 < z < 8$ . Such continuity has important implications for models of cosmic reionization and future searches for  $z > 10$  galaxies with JWST.

*Subject headings:* cosmology: reionization — galaxies: evolution — galaxies: formation — galaxies: stellar content

### 1. INTRODUCTION

Good progress has been achieved in recent years in exploring what many regard as the latest frontier in cosmic history, namely the 700 Myr period corresponding to the redshift interval  $6 < z < 15$ . During this time, star-forming galaxies may have played a significant role in completing the reionization of intergalactic hydrogen (Robertson et al. 2010a; Bromm & Yoshida 2011; Dunlop 2012). Inevitably, our census of galaxies during this era is limited by the power of our current observational facilities. Most progress has been made in the lower redshift range  $6 < z < 8.5$  via deep imaging with the *Hubble Space Telescope* (HST). This has revealed several hundred star-forming galaxies and a dominant contribution to the luminosity density from an abundant population of low luminosity examples (Oesch et al. 2010; McLure et al. 2011; Bouwens et al. 2010, 2012). Measures of the assembled stellar mass from Spitzer Space Telescope photometry at  $z \simeq 5-6$  (Stark et al. 2007a; Eyles et al. 2007; González et al. 2010, 2011; Labbé et al. 2012)

suggest that star formation extended to redshifts well beyond  $z \simeq 8$  but there has been limited progress in finding these earlier, more distant, sources.

Various groups have attempted to find  $8.5 < z < 10$  galaxies using the well-established technique of absorption by intervening neutral hydrogen below the wavelength of Lyman  $\alpha$ . A redshift  $z=8.5$  represents a natural frontier corresponding to sources which progressively ‘drop out’ in the HST Y-band F105W and J-band F125W filters. Bouwens et al. (2011) and Yan et al. (2010) used data from the HST campaign completed in 2009 with the near-infrared Wide Field Camera 3 (WFC3/IR) in the Hubble Ultra Deep Field (GO 11563, PI: Illingworth, hereafter UDF09). Bouwens et al. initially located 3 promising J-band dropout candidates at  $z \simeq 10$  but, on re-examining the completed dataset, presented only a single candidate, UDFj-39546284, not drawn from the original three. This source was detected with  $5.4 \sigma$  significance in the F160W filter and was undetected in all shorter wavelength HST images then available. A photometric redshift of  $z=10.3$  was proposed. Bouwens et al. also found 3 sources in the interval  $8.5 < z < 9$ , robustly detected in F125W with (F105W - F125W) colors greater than 1.5, implying a Lyman break near the red edge of the F105W filter. In marked contrast, Yan et al. presented a list of 20 faint J-band dropout candidates arguing these were likely at redshifts  $z > 8.5$ . However, none of the Yan et al. and Bouwens et al. candidates are in common.

Gravitational lensing by foreground clusters of galaxies can overcome some of the difficulties associated with deep imaging of blank fields. Such sources can be magnified by factors of  $\times 5-30$  ensuring more reliable photometry (Richard et al. 2011). In favorable cases, their multiply-imaged nature of-

<sup>1</sup> Department of Astrophysics, California Institute of Technology, MS 249-17, Pasadena, CA 91125; rse@astro.caltech.edu

<sup>2</sup> Institute for Astronomy, University of Edinburgh, Royal Observatory, Edinburgh EH9 3HJ, UK

<sup>3</sup> Department of Astronomy and Steward Observatory, University of Arizona, Tucson AZ 85721

<sup>4</sup> Institute for Cosmic Ray Research, University of Tokyo, Kashiwa City, Chiba 277-8582, Japan

<sup>5</sup> Space Telescope Science Institute, Baltimore, MD 21218

<sup>6</sup> Department of Physics & Astronomy, University of California, Los Angeles CA 90095

<sup>7</sup> IPRC-CNRS, UMR7095, Institut d’Astrophysique de Paris, F-75014, Paris, France

<sup>8</sup> UK Astronomy Technology Centre, Royal Observatory, Edinburgh EH9 3HJ, UK

fers a lower limit on their angular diameter distance (Ellis et al. 2001; Kneib et al. 2004). The CLASH HST survey (GO 12065 - 12791, PI: Postman) has discovered two such  $z > 8.5$  candidates. Zheng et al. (2012) present a source whose spectral energy distribution (SED) indicates a photometric redshift of  $z=9.6$  and Coe et al. (2012) located a multiply-imaged source whose SED indicates a redshift of  $z=10.7$ .

A key issue is the uncertainty in converting these single detections into an estimate of the overall abundance of galaxies beyond  $z \simeq 8$ . Bouwens et al. (2011, see also Oesch et al. (2012)) claimed that the detection of a single  $z \simeq 10.3$  candidate in the UDF09 campaign implies a shortfall of a factor  $\simeq 3-6$  compared to that expected from a smooth decline with redshift in the comoving star formation rate density over  $6 < z < 8$ . This could imply the growth of activity was particularly rapid during the 200 Myr from  $z \simeq 10$  to 8. However, Coe et al. (2012) claim the two CLASH detections are consistent with a continuous decline. One limitation of the lensing strategy as a means of conducting a census (rather than providing useful individual magnified sources for detailed scrutiny) is the uncertainty associated with estimating the survey volume which depends sensitively on the variation of magnification with position across the cluster field (c.f., Santos et al. 2004; Stark et al. 2007b).

There are several drawbacks with the earlier UDF09 campaign with respect to conducting a census of  $z > 8.5$  galaxies. Limiting factors in considering the robustness of the faint candidates include the poor signal to noise in subsets of the F160W data, the reliance on only a single detection filter and the limited depth of the critical F105W imaging data whose null detection is central to locating  $z > 8.5$  candidates.

This article heralds a series that presents results from a deeper UDF campaign with WFC3/IR completed in September 2012 (GO 12498, PI: Ellis, hereafter UDF12) which remedies the above deficiencies by (i) substantially increasing the depth of the F105W image (by  $\times 4$  in exposure time) essential for robust rejection of  $z < 8.5$  sources, (ii) increasing the depth of the detection filter F160W (a 50% increase in exposure time) and (iii) adding a deep image in the F140W filter matching the depth now attained in F160W. This filter partially straddles the F125W and F160W passbands offering valuable information on all  $z > 7$  sources, the opportunity for an independent detection for  $8.5 < z < 10.5$  sources and the first dropout search beyond  $z \simeq 10.5$ .

The UDF12 survey depths (including UDF09) in the various filters are summarized in Table 1. Our aim, achieved in full, has been to match the depths in F125W, F140W, and F160W for unbiased high redshift galaxy detection, and to reach 0.5 mag deeper in F105W to ensure a  $2\text{-}\sigma$  limit 1.5 mag deeper than the  $5\text{-}\sigma$  limit in the longer wavelength bands. Further details of the survey and its data reduction are provided in Koekemoer et al. (2012) and catalogs of  $z \simeq 7$  and 8 sources used to estimate the luminosity function are presented in complementary articles by Schenker et al. (2012) and McLure et al. (2012). The spectral properties of the high-redshift UDF12 sources are measured and analyzed by Dunlop et al. (2012). A review of the overall implications of the survey in the context of cosmic reionization is provided in Robertson et al. (2012). Public versions of the final reduced WFC3/IR UDF12 images, incorporating additions of all earlier UDF data, are available to the

community on the team web page<sup>9</sup>. All magnitudes are in the AB system (Oke 1974).

## 2. STAR FORMING GALAXIES WITH $Z > 8.5$

To select  $z > 8.5$  candidates, we examined the stacked combination of the final 80 orbit F160W (UDF12 plus UDF09), 30 orbit F140W (UDF12) and 34 orbit F125W (UDF09) images and located all sources to a  $5\sigma$  limit within filter-matched apertures of  $0.4 - 0.5$  arc sec corresponding to  $m_{AB} \simeq 29.9-30.1$ . Making effective use of our new ultra deep 93 orbit (71 from UDF12, 22 from UDF09) F105W image and the deep ACS photometry, we utilized the SED approach discussed in detail in McLure et al. (2010, 2011) to derive the photometric redshifts of all such sources. Seven convincing  $z > 8.5$  candidates were found. An independent search using the same master sample selecting those which drop out in F105W ( $2\sigma$  rejection corresponding to  $m_{AB} > 31.0$ ) and no detection ( $2\sigma$ ) in a combined ACS *BViz* stack delivered the same  $z > 8.5$  candidates. All sources but one (see below) are detected in more than one filter and all are detected with an appropriately-reduced signal/noise in time-split subsets over the collective UDF09 and UDF12 campaigns. Figure 1 shows the run of HST broad-band images with wavelength for these 7 sources and their SED fits and redshift probability distributions  $p(z)$  are given in Figure 2. Identifications, source photometry and optimum redshifts are summarized in Table 1.

The SED fitting approach allows us to quantify the possibility of alternative low-redshift solutions. Four objects (UDF12-3921-6322, UDF12-4265-7049, UDF12-4344-6547 & UDF12-3947-8076) have low probabilities of being at  $z < 4$  ( $1 - 4\%$ ). UDF12-4106-7304 is less secure with a  $\simeq 10\%$  probability for  $z < 4$ . This object also lies close to the diffraction pattern of an adjacent source which may affect the F140W photometry (Figure 1). UDF12-3895-7114 is the least secure with a 28% probability of lying at  $z < 4$ . We discuss UDF-3954-6284 in detail below.

Our deeper F105W data and the new F140W image enables us to clarify the nature of  $z > 8.5$  sources claimed in the earlier UDF09 analyses (see Table 1). In McLure et al. (2011)'s analysis of the UDF09 data, no robust *J*-band dropout source was claimed (see also Bunker et al. 2010). However a solution with  $z=8.49$  was found for HUDF\_2003 which was also listed as the brightest extreme *Y*-band dropout in Bouwens et al. (2011) (ID: UDFy-38135539) who inferred a redshift  $z \approx 8.7^{10}$ . Our new SED analysis indicates this source is at  $z=8.3$ . Similarly, two further extreme *Y*-band dropouts listed by Bouwens et al. (2011) - UDFy-37796000 and UDFy-33436598 at redshifts of  $z \approx 8.5$  and  $8.6$  now lie at  $z=8.0$  and  $7.9$ , respectively. Bouwens et al. (2011) initially presented 3 sources as promising *J*-band dropouts (see Table 1). Two of these are now detected in our deeper F105W data and lie at lower redshifts (UDFj-436964407 at  $z=7.6$  and UDFj-35427336 at  $z=7.9$ , although  $z \simeq 2$  solutions are also possible). One *Y*-band dropout in Bouwens et al. (2011), UDFy-39468075 moves into our sample at  $z=8.6$ . Finally, UDFj-38116243 claimed in the first year

<sup>9</sup> <http://udf12.arizona.edu/>

<sup>10</sup> This source was examined spectroscopically using the VLT SINFONI integral field spectrograph by Lehnert et al. (2010) who reported a detection of Ly $\alpha$  emission at  $z=8.6$  but this claim has been refuted by Bunker et al (in preparation) who undertook a separate spectroscopic exposure with the higher resolution spectrograph X-shooter.

UDF09 data but later withdrawn by Bouwens et al. (2011) is below our  $5\sigma$  detection limit. Yan et al. (2010) listed 20 potential  $J$ -band dropout candidates and an inspection of these revealed no convincing  $z > 8.5$  candidates. In our image stacks most appear as the tails of bright objects and cannot be reliably photometered by SeXtractor. And all of the ‘Y dropouts’ claimed by Lorenzoni et al. (2011) have robust F105W detections in our deeper data and lie well below  $z=8.5$ .

In summary, only one object claimed to be at  $z > 8.5$  from the entire UDF09 analysis remains convincing and that is the final  $J$ -band dropout presented by Bouwens et al. (2011) at  $z=10.3$ , UDFj-39546284 ( $\equiv$ UDF12-3954-6384 in Table 1). However, the absence of a detection in the new UDF12 F140W data for this source indicates a solution at a much higher redshift of  $z=11.9$  (Figure 2). The most significant advance of our campaign is a significant increase (from 0 to 6) in the number of robustly determined UDF sources in the redshift range  $8.5 < z < 10$ .

### 2.1. Contamination from Strong Emission Line Sources?

One of the motivations for the additional F140W filter in our UDF12 strategy was to ensure the robust detection in two filters of potential  $8.5 < z < 11.5$  candidates since the flux above  $1216 \text{ \AA}$  would be visible in both filters. Reassuringly, this is the case for all but one of our UDF12 candidates (Table 1). A major surprise however is the non-detection in F140W of UDFj-30546284 (Figures 1 and 2) implying a redshift of  $z=11.90$ .

Single band detections are naturally perceived as less convincing, although UDFj-30546284 is confirmed in F160W sub-exposures through UDF09 and UDF12, leaving no doubt it is a genuine source. However, a solution at much lower redshift has to be carefully considered. The sharp drop implied by the  $F140W - F160W > 1.5$  ( $2\sigma$ ) color precludes any reasonable foreground continuum source (Figure 2) but a possible explanation might be the presence of a very strong emission line. Recent WFC3/IR imaging and grism spectroscopy of intermediate redshift galaxies has revealed a population of extreme emission line galaxies (EELGs). van der Wel et al. (2011) have identified an abundant population of EELGs at  $z \simeq 1.7$  in the CANDELS survey using purely photometric selection techniques. Spectroscopic confirmation of a limited subset has verified the presence of sources with rest-frame [O III] equivalent widths larger than  $\simeq 200 \text{ \AA}$  and extending to  $\simeq 1000 \text{ \AA}$ . Independently, Atek et al. (2011) located a similar population in the WISP survey over a wider range  $0.35 < z < 2.3$  and comment specifically that such sources could contaminate dropout searches.

Following techniques described in Robertson et al. (2010a) and Ono et al. (2010), we have simulated model spectra for young low metallicity dust-free galaxies including the contribution from strong nebular lines. Figure 3a shows the expected F105W - F160W color as a function of redshift for starbursts with ages of 1 and 10 Myr demonstrating that it is not possible to account for the excess flux in F160W of which about 50-80% arises from [O III] 4959 and 5007  $\text{\AA}$  emission. Figure 3b illustrates that the expected stellar plus nebular emission spectrum of a 10 Myr starburst would violate upper photometric flux limits provided by the various ACS and WFC3/IR broad band non-detections. In the extreme case that all of the emission in F160W arises

from [O III] above a blue  $\beta=-2$  stellar continuum, the rest-frame equivalent width would be  $>4500 \text{ \AA}$ , i.e. beyond that of any known object. Unfortunately, only a spectrum would completely eliminate the possibility. As the source has  $H_{AB}=29.3$ , this would be a very challenging observation.

## 3. THE ABUNDANCE OF GALAXIES WITH $8.5 < Z < 12$

A key issue is whether the declining cosmic star formation which is now well-established over  $6 < z < 8$  (Bouwens et al. 2007) continues to higher redshift as suggested by the presence of evolved stellar populations with ages of  $\simeq 200$ -300 Myr at  $z \simeq 5$ -7 (e.g., Richard et al. 2011). Bouwens et al. (2011) claimed, from their detection of apparently only one object at  $z \simeq 10$  c.f. three expected, that the star formation history declines more steeply beyond  $z \simeq 8$  (see also Oesch et al. 2012) to  $\dot{\rho}_*(z \sim 10) \approx 2 \times 10^{-4} M_{\odot} \text{ yr}^{-1} \text{ Mpc}^{-3}$ . Recently, the CLASH survey has located candidates at  $z \approx 9.6$  (Zheng et al. 2012) and  $z \approx 10.7$  (Coe et al. 2012), each implying star formation rate densities approximately an order of magnitude higher than claimed by Bouwens et al. (2011) at  $z \sim 10$ . However, the uncertain search volumes inherent in the lensing method are a major concern.

In Figure 4 we present the implications of the significant increase in the number of  $8.5 < z < 12$  sources arising from the UDF12 campaign. Our SED-based selection method enables us to consider separately four redshift bins. As a direct determination of the luminosity function at  $z > 8.5$  is not yet possible, to estimate the ultraviolet luminosity densities for our four detections at  $8.5 \lesssim z < 9.5$  we calculate the required redshift evolution in the characteristic luminosity  $dM_*/dz$  such that a survey of our depth and selection efficiency would recover the number of sources we find. This calculation is performed assuming simple luminosity evolution from  $z \sim 8$ , keeping the luminosity function normalization  $\phi_*$  and faint-end slope  $\alpha$  fixed at the  $z \sim 8$  values measured by Bradley et al. (2012). To reproduce our sample with mean redshift  $\langle z \rangle \approx 8.9$ , we find that  $dM_*/dz \approx 1.01$ . The luminosity density can then be estimated by integrating the projected luminosity function parameters to  $M_{UV} \approx -17.7AB$  (e.g., Bouwens et al. 2011; Coe et al. 2012). We find  $\rho_{UV}(z \sim 8.9) \approx 1.18 \times 10^{25} \text{ ergs s}^{-1} \text{ Hz}^{-1} \text{ Mpc}^{-3}$  (Figure 4, blue point). A similar calculation provides  $\rho_{UV}(z \sim 9.8) \approx 8.34 \times 10^{24} \text{ ergs s}^{-1} \text{ Hz}^{-1} \text{ Mpc}^{-3}$  from the two  $z \sim 9.5$  detections (magenta point). The expected UDF cosmic variance for  $8.5 \lesssim z \lesssim 9.5$  is  $>40\%$  (Robertson 2010b). Within  $10.5 \lesssim z \lesssim 11.5$ , we find no candidates. Nonetheless we can use the same methodology to provide an upper limit of  $\rho_{UV}(z \sim 10.8) < 10^{25} \text{ ergs s}^{-1} \text{ Hz}^{-1} \text{ Mpc}^{-3}$  (Figure 4, purple upper limit).

Considering the putative  $z \sim 12$  source, we estimated the luminosity density only from the source luminosity ( $H_{160} = -19.6AB$  accounting for IGM absorption in F160W, or  $\log_{10} L_{UV} = 28.48 \log_{10} \text{ ergs s}^{-1} \text{ Hz}^{-1}$ ) and the UDF survey volume  $V(11.5 \lesssim z \lesssim 12.5) = 6.37 \times 10^3 \text{ Mpc}^3$ . The resulting luminosity density  $\rho_{UV}(z \sim 11.8) > 4.7 \times 10^{24} \text{ ergs s}^{-1} \text{ Hz}^{-1} \text{ Mpc}^{-3}$  is thus a lower limit (Figure 4, red point), and conservatively does not include multiplicative effects of selection efficiency or involve extrapolations from the  $z \sim 8$  luminosity function. An additional possibility is that the F160W is contaminated by Ly $\alpha$  emission. The

additional  $z=12$  point (yellow) illustrates how this limit would be affected for a rest-frame equivalent width of 260 Å of which half is absorbed by neutral hydrogen.

In summary, the new galaxy sample provided by UDF12 has enabled us to present the first meaningful estimate of  $\rho_{UV}(z)$  beyond  $z \simeq 8.5$ . The six galaxies with  $8.5 < z < 10$  indicate a modest shortfall in  $\rho_{UV}(z)$  beyond a simple extrapolation of the trend at  $6 < z < 8$  (less sharp than that suggested by Bouwens et al. (2011), but below (albeit consistent with) the cluster results (Zheng et al. 2012; Coe et al. 2012)). However, if UDFj-30546284 is genuinely a  $z=12$  galaxy (and does not have substantial Lyman- $\alpha$  emission) then we have witnessed an even more measured decline in  $\rho_{UV}(z)$  to the highest redshift yet probed.

#### 4. DISCUSSION

The UDF12 data has clearly demonstrated the continued effectiveness of HST to uniquely undertake a census of very high redshift galaxies. Our discovery of the first robust sample of galaxies with  $z > 8.5$  and new evidence for the most distant known galaxy at  $z \sim 12$  extends HST's reach further into the reionization epoch than previously thought possible (c.f., Bouwens et al. 2011). While the question of whether star-forming galaxies were solely responsible for reionizing intergalactic hydrogen is more reliably addressed through precise constraints on the  $z \sim 7-8$  luminosity function faint end slope (Schenker et al. 2012; McLure et al. 2012, for a new analysis, see Robertson et al. 2012) this

work has placed the first constraint on the SFR density only 360 million years after the Big Bang. Evidence for actively star-forming galaxies significantly beyond the instantaneous reionization redshift  $z_{\text{reion}} \approx 10.6 \pm 1.2$  implied by observations of the cosmic microwave background (Komatsu et al. 2011) motivates future observations with *James Webb Space Telescope*. Our estimates of the  $z \sim 12$  luminosity and star formation rate densities are consistent with the inferences of previous analyses that aim to explain the measured Thomson optical depth (e.g. Robertson et al. 2010a; Kuhlen & Faucher-Giguère 2012). Similarly, our  $z \sim 12$  discovery is consistent with star formation rate history required to produce the stellar mass inferred for  $z < 8$  sources observed by *Spitzer* (e.g., Stark et al. 2012; Labbé et al. 2012). Our results remain consistent with the simple picture for the evolving star formation rate density, stellar mass density, Thomson optical depth, and IGM ionization fraction presented in Robertson et al. (2010a).

US authors acknowledge financial support from the Space Telescope Science Institute under award HST-GO-12498.01-A. JSD acknowledges support of the European Research Council and the Royal Society. RJM acknowledges funding from the Leverhulme Trust. This work is based on data from the *Hubble Space Telescope* which is operated by NASA through the Space Telescope Science Institute via the association of Universities for Research in Astronomy, Inc. for NASA under contract NAS5-26555.

#### REFERENCES

- Atek, H., et al. 2011, *ApJ*, 743, 121  
 Bouwens, R. J., Illingworth, G. D., Franx, M., & Ford, H. 2007, *ApJ*, 670, 928  
 Bouwens, R. J., et al. 2011, *Nature*, 469, 504  
 —. 2010, *ApJ*, 709, L133  
 —. 2012, *ApJ*, 752, L5  
 Bradley, L. D., et al. 2012, arXiv:1204.3937  
 Bromm, V., & Yoshida, N. 2011, *ARA&A*, 49, 373  
 Bunker, A. J., et al. 2010, *MNRAS*, 409, 855  
 Calzetti, D., Armus, L., Bohlin, R. C., Kinney, A. L., Koornneef, J., & Storchi-Bergmann, T. 2000, *ApJ*, 533, 682  
 Coe, D., et al. 2012, submitted  
 Dunlop, J. S. 2012, ArXiv: 1205.1543  
 Dunlop, J. S., et al. 2012, in preparation  
 Ellis, R., Santos, M. R., Kneib, J.-P., & Kuijken, K. 2001, *ApJ*, 560, L119  
 Eyles, L. P., Bunker, A. J., Ellis, R. S., Lacy, M., Stanway, E. R., Stark, D. P., & Chiu, K. 2007, *MNRAS*, 374, 910  
 González, V., Labbé, I., Bouwens, R. J., Illingworth, G., Franx, M., & Kriek, M. 2011, *ApJ*, 735, L34  
 González, V., Labbé, I., Bouwens, R. J., Illingworth, G., Franx, M., Kriek, M., & Brammer, G. B. 2010, *ApJ*, 713, 115  
 Kneib, J.-P., Ellis, R. S., Santos, M. R., & Richard, J. 2004, *ApJ*, 607, 697  
 Koekemoer, A., et al. 2012, in preparation  
 Komatsu, E., et al. 2011, *ApJS*, 192, 18  
 Kuhlen, M., & Faucher-Giguère, C.-A. 2012, *MNRAS*, 423, 862  
 Labbe, I., et al. 2012, ArXiv e-prints  
 Lehnert, M. D., et al. 2010, *Nature*, 467, 940  
 Lorenzoni, S., et al. 2011, *MNRAS*, 414, 1455  
 Madau, P., Pozzetti, L., & Dickinson, M. 1998, *ApJ*, 498, 106  
 McLure, R. J., Dunlop, J. S., Cirasuolo, M., Koekemoer, A. M., Sabbi, E., Stark, D. P., Targett, T. A., & Ellis, R. S. 2010, *MNRAS*, 403, 960  
 McLure, R. J., et al. 2011, *MNRAS*, 418, 2074  
 McLure, R. J., et al. 2012, in preparation  
 Oesch, P. A., et al. 2010, *ApJ*, 709, L16  
 —. 2012, *ApJ*, 745, 110  
 Oke, J. B., 1974 *ApJS*, 27, 21  
 Ono, Y., Ouchi, M., Shimasaku, K., Dunlop, J., Farrah, D., McLure, R., & Okamura, S. 2010, *ApJ*, 724, 1524  
 Richard, J., Kneib, J.-P., Ebeling, H., Stark, D. P., Egami, E., & Fiedler, A. K. 2011, *MNRAS*, 414, L31  
 Robertson, B. E., Ellis, R. S., Dunlop, J. S., McLure, R. J., & Stark, D. P. 2010, *Nature*, 468, 49  
 Robertson, B. E. 2010, *ApJ*, 713, 1266  
 Robertson, B., et al. 2012, in preparation  
 Santos, M. R., Ellis, R. S., Kneib, J.-P., Richard, J., & Kuijken, K. 2004, *ApJ*, 606, 683  
 Schenker, M., et al. 2012, in preparation  
 Shapley, A. E., Steidel, C. C., Pettini, M., & Adelberger, K. L. 2003, *ApJ*, 588, 65  
 Stark, D. P., Bunker, A. J., Ellis, R. S., Eyles, L. P., & Lacy, M. 2007a, *ApJ*, 659, 84  
 Stark, D. P., Ellis, R. S., Richard, J., Kneib, J.-P., Smith, G. P., & Santos, M. R. 2007b, *ApJ*, 663, 10  
 Stark, D. P., Schenker, M. A., Ellis, R. S., Robertson, B., McLure, R., & Dunlop, J. 2012, ArXiv e-prints  
 van der Wel, A., et al. 2011, *ApJ*, 742, 111  
 Yan, H.-J., Windhorst, R. A., Hathi, N. P., Cohen, S. H., Ryan, R. E., O'Connell, R. W., & McCarthy, P. J. 2010, *Research in Astronomy and Astrophysics*, 10, 867  
 Zheng, W., et al. 2012, *Nature*, 489, 406

TABLE 1  
 $z > 8.5$  Candidates

ID	RA	Dec	$z_{\text{SED}}$	$Y_{105W}$	$J_{125W}$	$J_{140W}$	$H_{160W}$	Notes
<b>UDF12 Survey Depth 5-<math>\sigma</math> AB (aperture diameter arcsec - 70% enclosed point source flux)</b>								
				30.0 (0.40)	29.5 (0.44)	29.5 (0.47)	29.5 (0.50)	
<b>UDF12 Galaxies</b>								
UDF12-3954-6284	3:32:39.54	-27:46:28.4	11.9	< 31.2	< 30.7	< 30.5	$29.3 \pm 0.2$	UDFj-39546284(Bouwens et al 2011)
UDF12-4106-7304	3:32:41.06	-27:47:30.4	9.5	< 30.8	< 30.0	$29.8 \pm 0.3$	$29.7 \pm 0.3$	
UDF12-4265-7049	3:32:42.65	-27:47:04.9	9.5	< 31.2	$30.4 \pm 0.6$	$29.9 \pm 0.4$	$29.7 \pm 0.4$	
UDF12-3921-6322	3:32:39.21	-27:46:32.2	8.8	< 31.2	$29.9 \pm 0.3$	$29.6 \pm 0.3$	$29.9 \pm 0.3$	
UDF12-4344-6547	3:32:43.44	-27:46:54.7	8.7	< 31.2	$30.0 \pm 0.3$	$30.1 \pm 0.4$	$30.1 \pm 0.3$	
UDF12-3895-7114	3:32:38.95	-27:47:11.4	8.6	< 30.9	$30.4 \pm 0.5$	$30.1 \pm 0.3$	$30.1 \pm 0.4$	
UDF12-3947-8076	3:32:39.47	-27:48:07.6	8.6	$31.0 \pm 0.5$	$29.5 \pm 0.2$	$29.0 \pm 0.1$	$29.0 \pm 0.1$	UDFy-39468075(Bouwens et al 2011)
<b>Earlier Candidates</b>								
UDFj-39546284	3:32:39.54	-27:46:28.4	11.9	< 31.2	< 30.7	< 30.5	$29.3 \pm 0.2$	Bouwens et al (2011) $z \approx 10.3$
UDFj-38116243	3:32:38.11	-27:46:24.3	—	< 31.2	< 30.1	$30.3 \pm 0.5$	$30.0 \pm 0.3$	Bouwens et al UDF09 yr 1 #1, yr 2 #2
UDFj-43696407	3:32:43.69	-27:46:40.7	7.6	$31.0 \pm 0.6$	< 30.1	$29.9 \pm 0.3$	$29.5 \pm 0.2$	Bouwens et al UDF09 yr 1 #2
UDFj-35427336	3:32:35.42	-27:47:33.6	7.9	< 30.8	$30.3 \pm 0.4$	$30.2 \pm 0.4$	$29.6 \pm 0.2$	Bouwens et al UDF09 yr 1 #3
UDFy-38135539	3:32:38.13	-27:45:53.9	8.3	$30.1 \pm 0.2$	$28.6 \pm 0.1$	$28.5 \pm 0.1$	$28.4 \pm 0.1$	Bouwens et al (2011) $8.5 < z < 9.5$
UDFy-37796000	3:32:37.79	-27:46:00.0	8.0	$29.8 \pm 0.1$	$28.6 \pm 0.1$	$28.7 \pm 0.1$	$28.7 \pm 0.1$	Bouwens et al (2011) $8.5 < z < 9.5$
UDFy-33436598	3:32:33.43	-27:46:59.8	7.9	$30.3 \pm 0.4$	$29.3 \pm 0.2$	$29.4 \pm 0.2$	$29.4 \pm 0.1$	Bouwens et al (2011) $8.5 < z < 9.5$

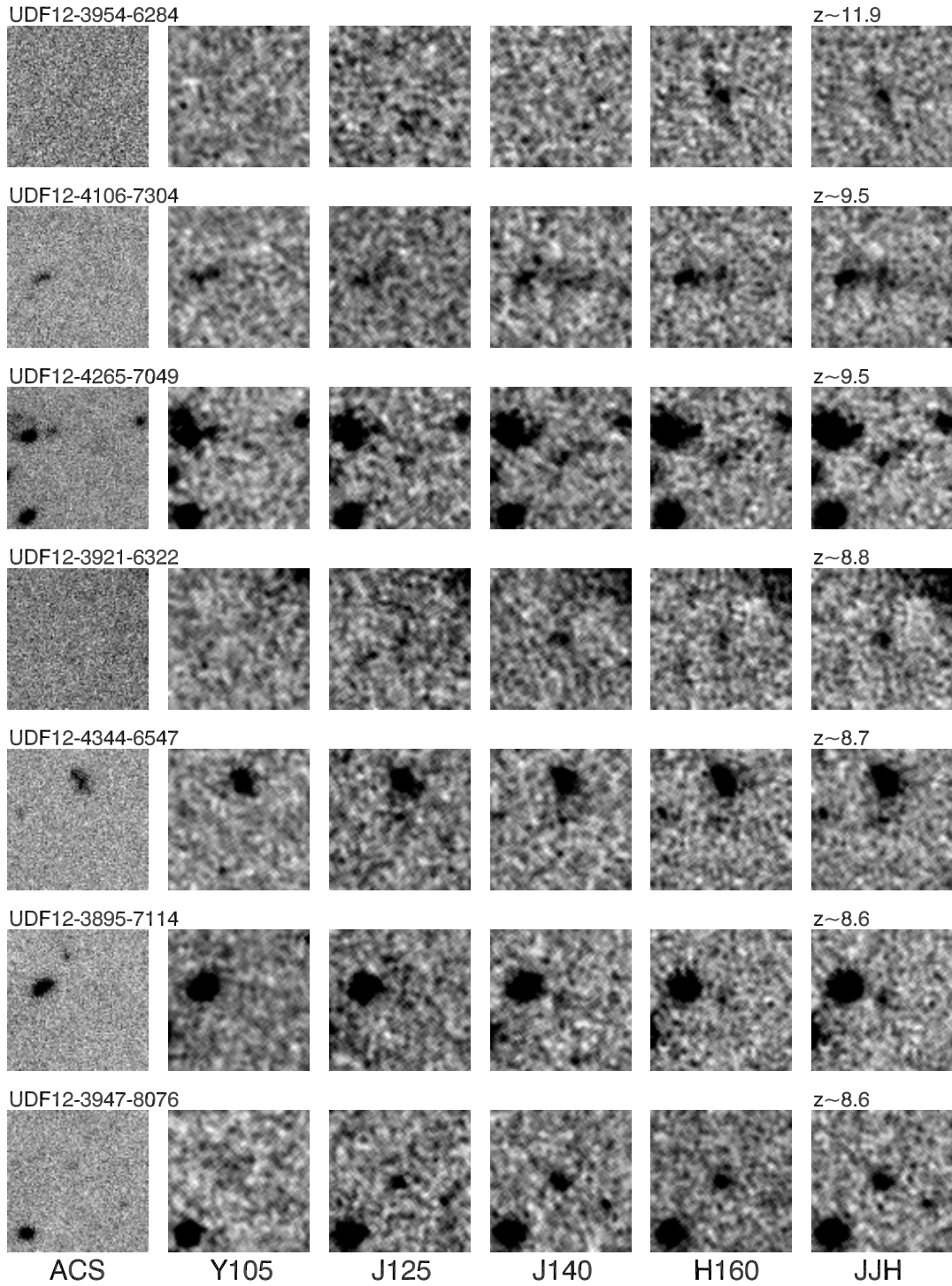


FIG. 1.— Hubble Space Telescope images of the 7 promising  $z > 8.5$  candidates from the combined UDF12 and earlier data. Each panel is 2.4 arcsec on a side. From left to right: combined BViz ACS stack, WFC3/IR F105W, F125W, F140W, F160W and the summed (F125W+F140W+F160W) stack.

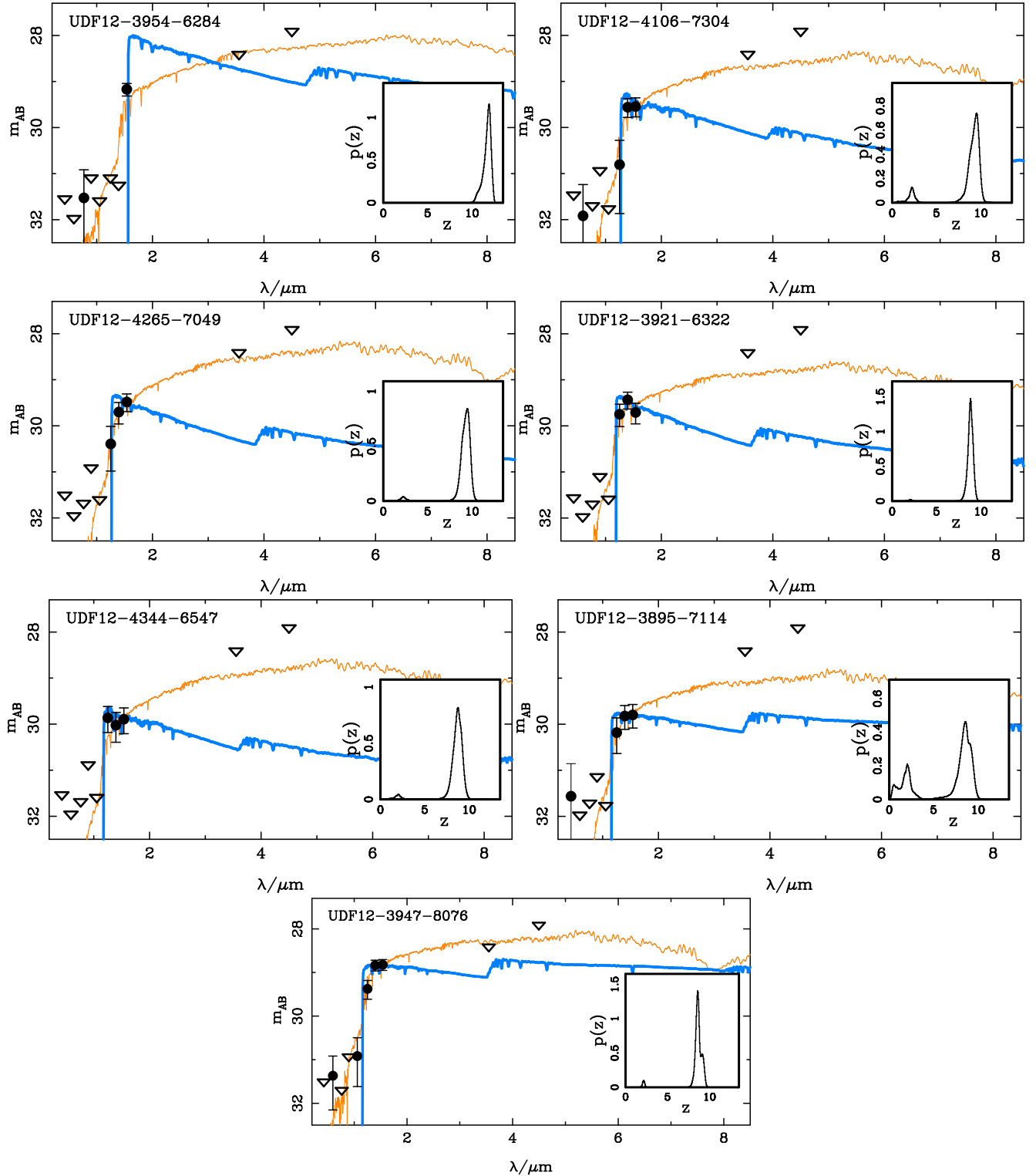


FIG. 2.— Spectral energy distributions and photometric likelihood fits for the 7 promising  $z > 8.5$  candidates from the combined UDF12 and earlier data. IRAC limits are derived from a deconvolution analysis of the data from Labbé et al. (2012).

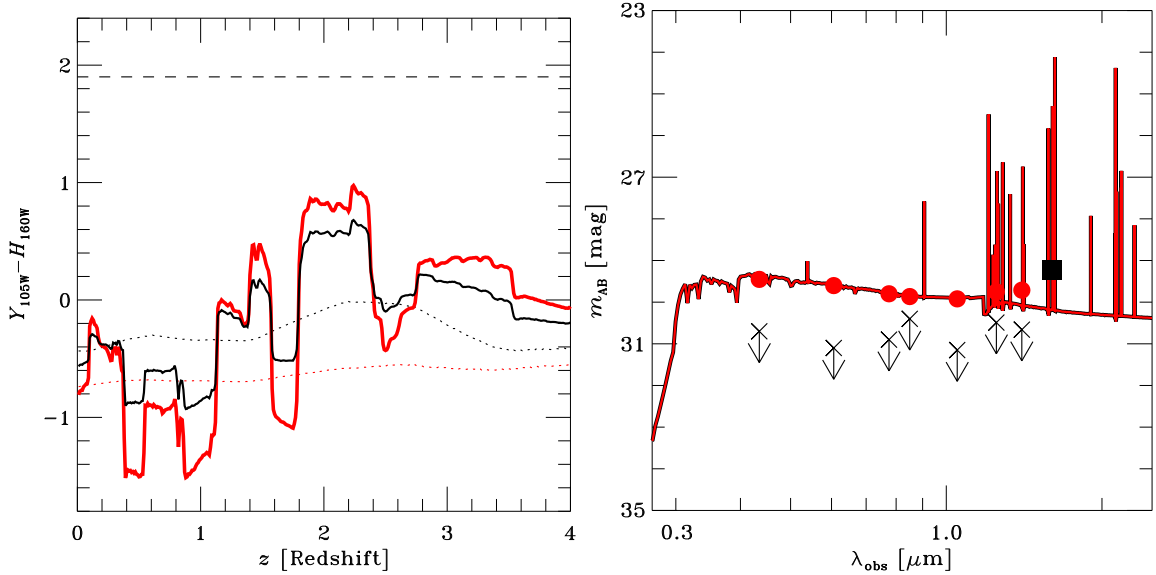


FIG. 3.— Possible contamination of WFC3/IR passbands by foreground extreme emission line galaxies. (Left) F105W minus F160W color as a function of redshift for a 1 Myr (red line) and 10 Myr (black line) metal-poor dust-free stellar population incorporating nebular line emission according to the precepts discussed by Ono et al (2010). The color expected for a stellar continuum only is shown by the lower dotted lines. The upper dashed line shows the lower limit for UDFj-39546284 derived from the overall  $2\sigma$  F105W limit minus the source's  $>6\sigma$  F160W detection. (Right). Simulated spectrum ( $AB_\lambda$ ) of UDFj-39546284 for a 10 Myr starburst at  $z=2.24$ . Arrows indicate the  $2\sigma$  upper limits arising from non-detections of this object in the various WFC3/IR and ACS bands. This indicates that UDFj-39546284 is unlikely to be a foreground line emitter.

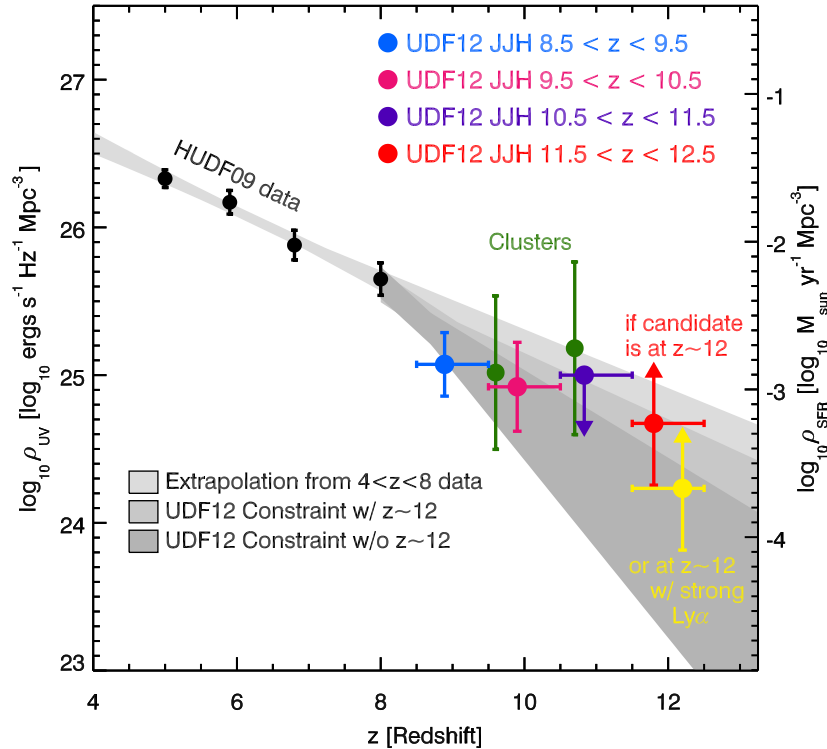


FIG. 4.— Luminosity and star formation rate (SFR) density versus redshift inferred from UDF12. Reddening corrected luminosity densities are shown from Bouwens et al. (2007, 2011) over the redshift range  $5 < z < 8$  (black points). Extrapolating their evolution to redshift  $z \sim 13$  provides the lightest gray area. Claimed estimates from the single CLASH detections (green points) at  $z=9.6$  (Zheng et al. 2012) and  $z=10.7$  (Coe et al. 2012) are shown for completeness. The luminosity and SFR densities supplied by the four  $8.5 \lesssim z \lesssim 9.5$  sources (blue data point) and the two  $9.5 \lesssim z \lesssim 10.5$  objects (magenta point). The nondetection at  $10.5 \lesssim z \lesssim 11.5$  provides an upper limit at  $z \approx 10.8$  (purple limit). The single  $z \sim 12$  source provides the conservative lower limit at  $z \approx 11.8$  as indicated (red point). If the  $z \sim 12$  system has strong Ly $\alpha$  emission, the  $z \sim 12$  luminosity density moves to the yellow point. Overlapping maximum likelihood 68% confidence regions on a linear trend in the luminosity density with redshift from  $z \sim 8$  are shown with (medium gray) and without (dark gray) including the  $z \sim 12$  object. The luminosity density computation is described in Section 3. Star formation rates were calculated using the conversion of Madau et al. (1998).